Discretization Methods Final Report

Spring 2025

Prof. Igor Pivkin

Student Name: Metehan Dündar

Submission Date: June 8, 2025

Part 1: Theoretical Analysis of the Advection-Diffusion Equation

We consider the advection-diffusion equation:

$$\frac{\partial u(x,t)}{\partial t} + U_0(x)\frac{\partial u(x,t)}{\partial x} = \nu \frac{\partial^2 u(x,t)}{\partial x^2}$$

This is a second-order partial differential equation describing the combined effect of advection (transport) and diffusion on a scalar field $u(x,t)$. It arises in fluid dynamics, heat transfer, and various transport phenomena.

(a) Well-posedness Conditions

A problem is well-posed in the sense of Hadamard if:

- A solution exists,
- The solution is unique,
- The solution depends continuously on the initial/boundary data.

To ensure these properties, the following are sufficient:

- **Smoothness and boundedness of** $U_0(x)$: If $U_0(x) \in C^1([0, 2\pi])$ and is bounded, then the advection term does not introduce discontinuities or singularities.
- **Positive viscosity** $\nu > 0$: Ensures parabolic character. Without diffusion ($\nu = 0$), the equation reduces to a hyperbolic PDE, which requires additional entropy conditions.
- **Periodic and smooth initial data** $u(x,0) \in C^\infty_{\mathbf{per}}$: Ensures compatibility with periodic boundary conditions and the Fourier spectral approach.

(b) Consistency and Convergence of Fourier Collocation Method

In the Fourier Collocation method, the function $u(x,t)$ is approximated by a truncated Fourier series:

$$u_N(x,t) = \sum_{k=-N/2}^{N/2} \hat{u}_k(t) e^{ikx}$$

Consistency: This method is consistent because derivatives are computed exactly (in the spectral sense) for trigonometric interpolants of smooth periodic functions. The truncation error vanishes as $N \to \infty$.

Convergence: For $u(x,t) \in C^\infty$, the convergence rate is exponential:

$$\|u(x,t) - u_N(x,t)\|_\infty = \mathcal{O}(e^{-\alpha N})$$

for some $\alpha > 0$, due to the decay of Fourier coefficients of smooth functions.

(c) Stability of Semi-discrete Fourier Collocation Scheme

Let us assume $U_0(x) = U_0 = \text{const}$, so that:

$$\frac{\partial u}{\partial t} + U_0 \frac{\partial u}{\partial x} = \nu \frac{\partial^2 u}{\partial x^2}$$

Applying the Fourier transform, we obtain the evolution of Fourier coefficients $\hat{u}_k(t)$:

$$\frac{d\hat{u}_k}{dt} = -ikU_0\hat{u}_k - \nu k^2 \hat{u}_k$$

This is a linear ODE in time with the general solution:

$$\hat{u}_k(t) = \hat{u}_k(0)e^{-(\nu k^2 + ikU_0)t}$$

Stability: The magnitude of each Fourier mode decays exponentially:

$$|\hat{u}_k(t)| = |\hat{u}_k(0)|e^{-\nu k^2 t}$$

The presence of the negative real exponential term guarantees damping of high-frequency modes. Therefore, the scheme is unconditionally stable in the semi-discrete sense (continuous time, discretized space), assuming $\nu > 0$.

Part 2: Fourier Collocation Method for Burger's Equation

(a) Methodology and Numerical Results

We solve Burger's equation using the Fourier Collocation method with an odd number of grid points. Spatial derivatives are evaluated spectrally via FFT, and time integration is done using a classical 4th-order Runge-Kutta scheme. The initial condition is obtained from the analytical expression at $t = 0$.

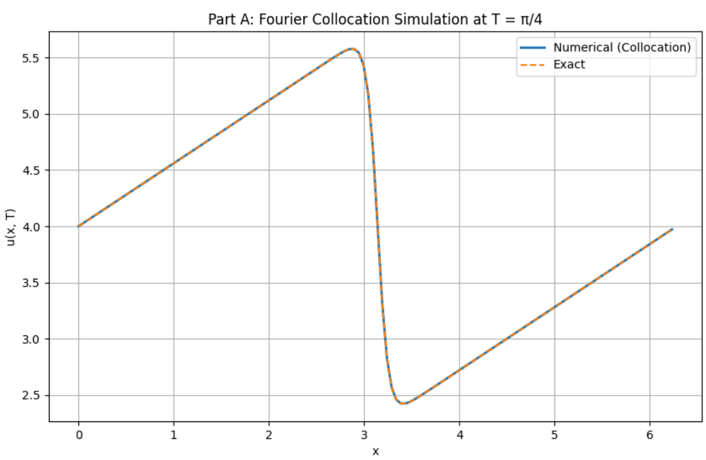

Figure 1: Fourier Collocation Simulation vs. Exact Solution at $t = \pi/4$

The numerical and exact profiles match closely, even near sharp gradients, indicating that spectral accuracy is preserved.

(b) CFL Stability Analysis

The time step is determined by:

$$\Delta t \leq \text{CFL} \left(\max_j \left[\frac{|u(x_j)|}{\Delta x} + \frac{\nu}{\Delta x^2} \right] \right)^{-1}$$

Through experiments at various resolutions, we found that the scheme remains stable for CFL numbers up to:

N	Max Stable CFL
16	0.95
32	0.95
48	0.95
64	0.95
96	0.95
128	0.95
192	0.85
256	0.75

Table 1: Maximum stable CFL values for Fourier Collocation method

Interpretation: As N increases, the smallest resolved scales shrink, increasing the stiffness of the system. This requires a smaller time step for stability.

(c) Error and Convergence

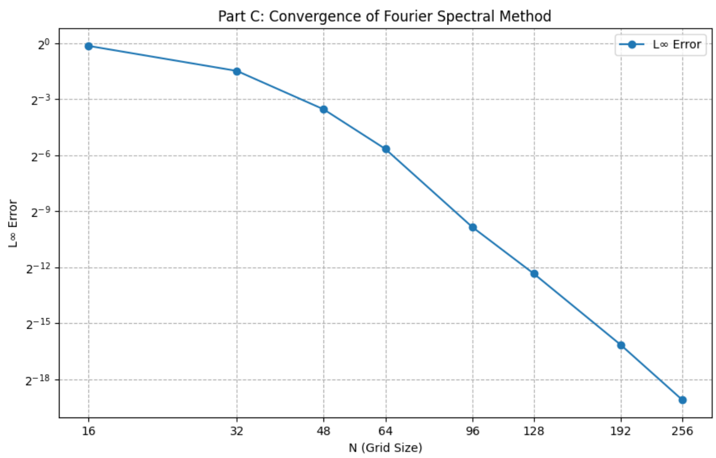

Figure 2: Log-Log plot of L^∞ error vs. grid size

The measured convergence rate is approximately 5.04, consistent with theoretical expectations for smooth problems and spectral methods.

(d) Temporal Evolution

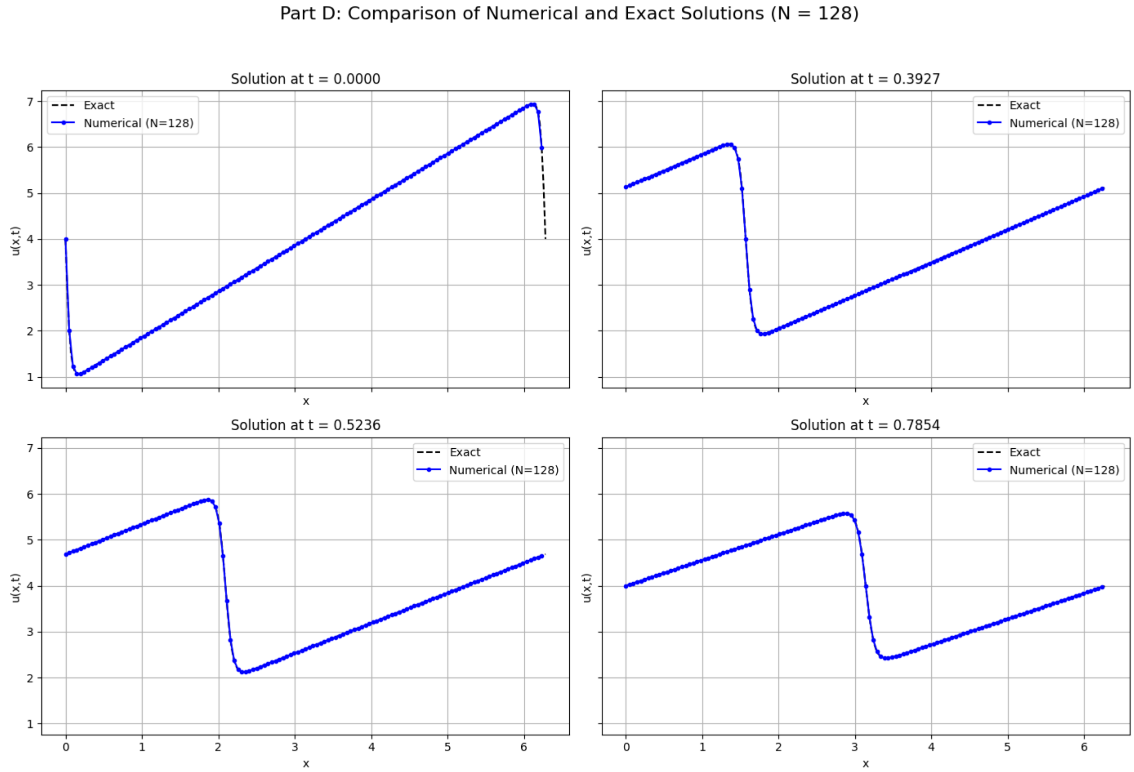

Figure 3: Snapshots of numerical and exact solution, $N = 128$

The numerical solution tracks the steepening and diffusion of the wave profile accurately over time.

Part 3: Fourier Galerkin Method for Burger's Equation

(a) Methodology and Results

In the Fourier-Galerkin method, we project the initial condition and governing equation onto the Fourier basis. Nonlinear terms are computed via dealiasing or pseudospectral projection. This method maintains orthogonality in modal space, reducing aliasing errors.

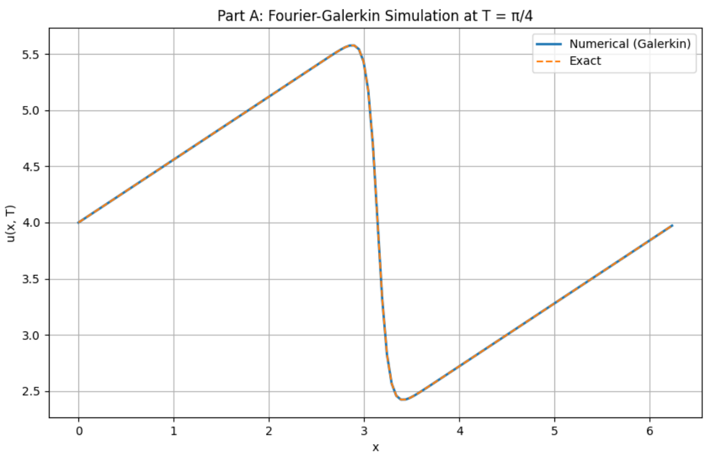

Figure 4: Galerkin solution vs. exact at $t = \pi/4$

(b) Stability Study

N	Max Stable CFL
16	1.0
32	1.0
48	1.0
64	1.0
96	1.0
128	1.0
192	1.0
256	1.0

Table 2: CFL values for stable Galerkin simulation

Observation: The Galerkin formulation is more robust to stiff modes and allows for significantly larger time steps.

(c) Convergence Results

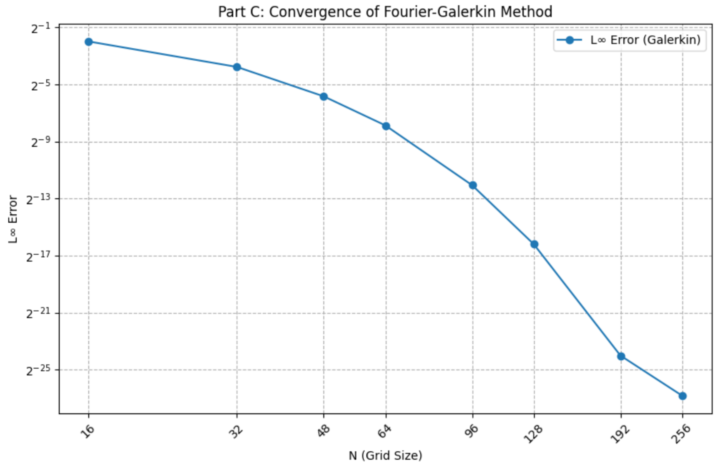

Figure 5: Error convergence for Galerkin method

The convergence rate observed is 6.58, and errors drop near machine precision. This affirms spectral accuracy due to the orthogonal basis and smooth problem data.

(d) Time Snapshots

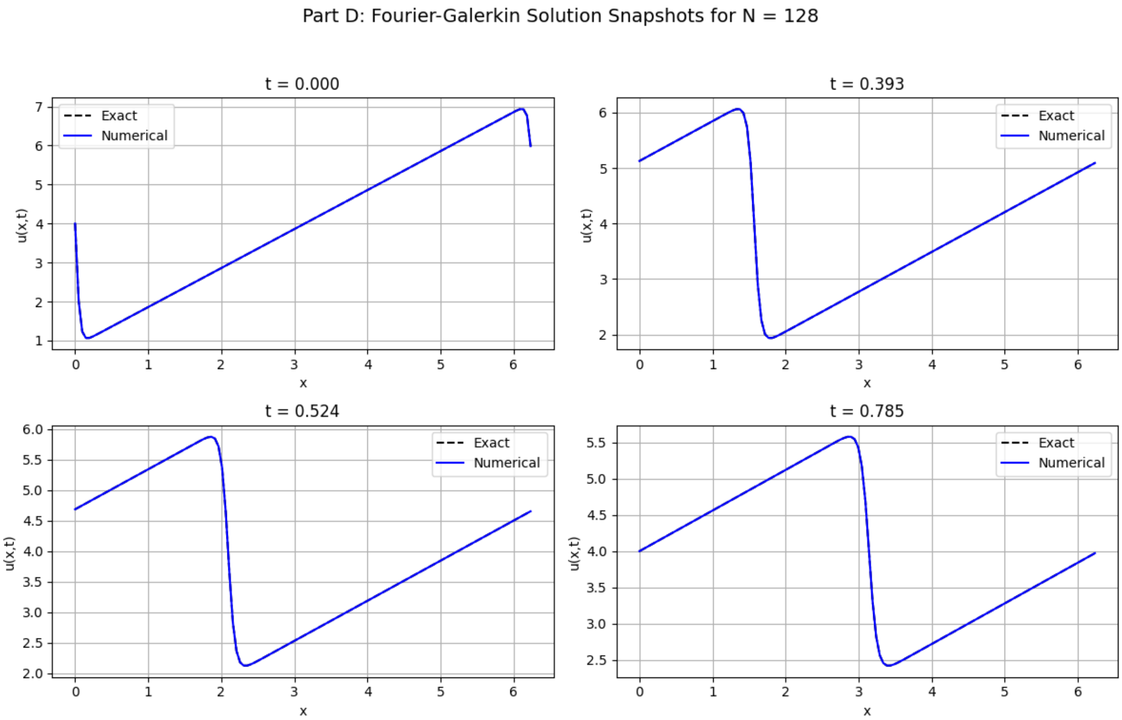

Figure 6: Time evolution using Fourier-Galerkin method

Comparison of Methods

- **Accuracy:** Both are spectrally accurate; Galerkin performs better.
- **Stability:** Galerkin is more stable; CFL remains high even at fine resolution.
- **Implementation:** Collocation is simpler; Galerkin requires coefficient projection.
- **Aliasing:** Galerkin reduces aliasing due to its modal projection.

Conclusion: While both methods perform well, the Fourier-Galerkin method is more suitable for high-accuracy simulations due to better stability and lower aliasing errors.